

# INITIAL STUDY ON SMALL DEBRIS IMPACT RISK ASSESSMENT DURING ORBIT TRANSFER TO GEO FOR ALL-ELECTRIC SATELLITE

Masumi Higashide<sup>(1,2)</sup>, Martin Schimmerohn<sup>(2)</sup>, Frank Schäfer<sup>(2)</sup>

<sup>(1)</sup> Japan Aerospace Exploration Agency, 7-44-1 Jindaiji Higashimachi, Chofu, Tokyo, JAPAN,  
Email: higaside@chofu.jaxa.jp

<sup>(2)</sup> Fraunhofer Institute for High-Speed Dynamics, Ernst-Mach-Institut, Eckerstrasse 4, Freiburg, GERMANY,  
Email: Martin.Schimmerohn@emi.fraunhofer.de, Frank.Schaefer@emi.fraunhofer.de

## ABSTRACT

This study has investigated the risk of small debris impacting a satellite during orbit transfer from geostationary transfer orbit to geostationary earth orbit. The risks during orbit transfer by conventional chemical propulsion are compared with those by electric propulsion. As orbit transfer by electric propulsion needs a few months, 180 days are assumed for the transfer. The impact frequencies of each component have been analyzed for a three-dimensional satellite model by using an impact risk assessment tool. The impact frequencies on the components become higher in line with a longer transfer duration. The risk estimated by single surface fluxes calculated by MASTER-2009 has been also evaluated. The estimation was found to have overestimated the risk.

## 1 INTRODUCTION

Satellites in geostationary earth orbit (GEO) are expected to increase their electric power. Almost all GEO satellites have several thrusters, one used for transfer from launched orbit to GEO, and others used for attitude control. The collective weight of these thrusters accounts for about half of the launch weight. To increase the dry weight of a GEO satellite, focus is placed on an electric propulsion technique. The electric propulsion system is well-known for its high specific thrust. The Eutelsat 115 West B and ABS-3A launched in March 2015 were successfully transferred to GEO with only electric propulsion thrusters. In both cases, orbit transfer required six months. Since the electric propulsion system has thrust force smaller than that of chemical propulsion, the duration of orbit transfer entails several months when only electric propulsion is used for transfer to GEO. Consequently, the satellite will remain in orbit (including areas having a high density of space debris) for a longer time compared to transfer by chemical propulsion. Therefore, the risk of debris impacting an electric propulsion satellite should be higher than the risk for a chemical propulsion satellite.

Debris impact damage to satellites can be categorized as catastrophic or non-catastrophic. Catastrophic damage is

caused by larger debris (greater than several cm in size). Many fragments are produced from a catastrophic collision [1,2], that is, the debris environment becomes far worse due to a catastrophic collision. Conversely, a non-catastrophic collision does not produce large fragments. However, non-catastrophic damage can induce the functional loss of specific components, a reduction in solar power, and other adverse effects [3,4]. Such damage is caused by smaller debris impacts. Therefore, non-catastrophic damage occurs more frequently than catastrophic damage. This study focuses on non-catastrophic damage. The purpose of this study is to assess the risk of non-catastrophic damage to a satellite transferring from geostationary transfer orbit (GTO) to GEO with only electric propulsion thrusters.

## 2 ANALYSIS CONDITIONS

### 2.1 Orbit

A duration of 180 days (approximately 6 months) was set for transferring from GTO to GEO. The transfer orbit was assumed as shown in Fig. 1. The initial orbit is 300 km at apogee, 35,800 km at perigee, and 25° in inclination. The satellite is finally located in GEO (altitude of 35,800 km and inclination of 0°). The altitude of perigee is expressed

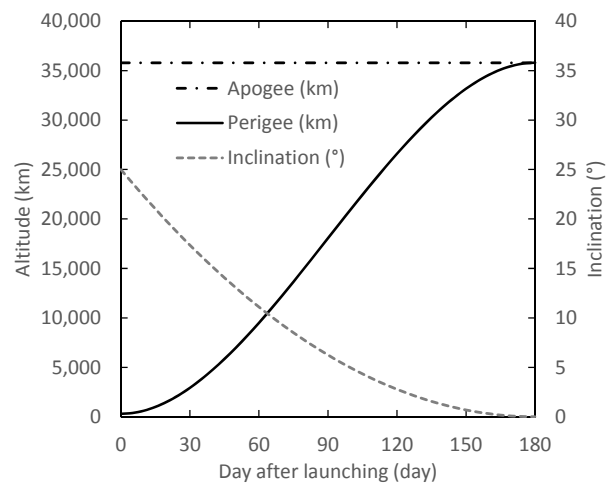


Figure 1. Assumed Transfer Orbit

as a cubic equation, assuming that the satellite goes through the half point (17,750 km) on the 90th day. The inclination is expressed as a quadratic equation.

## 2.2 Satellite Model

Fig. 2 shows the satellite model used in this study. This model was developed based on the Boeing 702SP bus that is employed for all-electric satellites now in orbit. The main structure measures 2 m × 2 m × 3.5 m in size. Two pairs of two Ion thrusters (0.25 m in diameter) are installed on the north and south surfaces, respectively. Four solar array panels (SAPs) measuring 2 m × 4 m are connected and expanded in the leading and trailing directions. The shape of the SAP arm is modelled as a box measuring 0.1 m × 0.1 m × 1.1 m. To simulate a satellite transferring to GEO, two antennas (2.5 m in diameter) are installed on the structure panels. A propellant tank (1 m in diameter, 1.5 m in height) is installed inside the main structure. To assess the risk of debris impacting payloads, four boxes are also put inside the structure. The two boxes located in the zenith direction measure 0.2 m × 0.5 m × 0.25 m in size; the other two measure 0.95 m × 0.45 m × 1.45 m.

## 3 RISK ASSESSMENT BY MASTER-2009

Fluxes of particles impacting the satellite were calculated by MASTER-2009. The flux in 2015 was used in this study. The fluxes impacting during an orbit transfer are compared between electric and chemical propulsions. Transfer with chemical propulsion is assumed to take three days. In the chemical propulsion scenario, the initial orbit is the same as described in Section 2.1. A satellite's

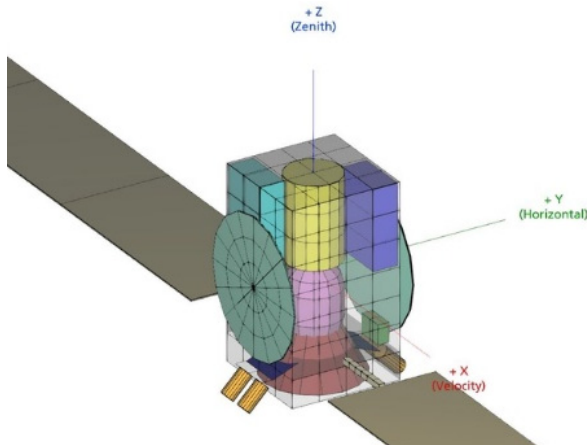


Figure 2. Satellite Model

Table 1. Impact Flux during Orbit Transfer

Object Diameter	Flux (1/m <sup>2</sup> )	
	Electric	Chemical
> 1 μm	1690	28.9
> 0.1 mm	3.64	0.0650
> 1 mm	0.00184	0.0000315

perigee is moved to approximately 7,000 km on the 1st day and to approximately 28,000 km on the 2nd day. The satellite reaches GEO on the 3rd day. Tab. 1 shows the total impact fluxes during orbit transfer. The total flux of an electric propulsion transfer is about 60 times higher than that of a chemical propulsion transfer. This value is almost the same as the ratio of increase in transfer durations.

To estimate the impact risk for satellite components, fluxes passing through single surfaces have been calculated by MASTER-2009. As an example, Fig. 3 shows the impact fluxes of particles larger than 0.1 mm in diameter. The leading surface has the highest risk; the trailing surface has the lowest risk. The fluxes of other particle diameters have showed the same trend. By using these fluxes, the particle impact frequencies of each satellite component have been estimated from the projected area of the component onto each surface shown in Fig. 3. Tab. 2 shows the calculated impact frequencies. The frequencies of antennas, solar array cells, SAP arms, and thrusters indicate the sum of these components. The impact frequency of particles larger than 1 μm is more

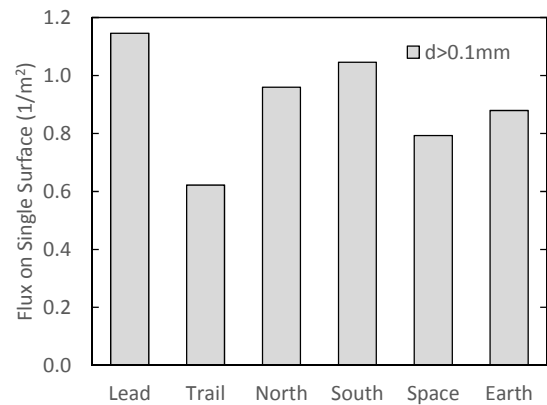


Figure 3. Flux of Particles Larger than 0.1 mm Impacting on Single Surfaces

Table 2. Component Impact Risks Estimated from Single Surface Fluxes\

Component	Impact Frequency		
	> 1 μm	> 0.1 mm	> 1 mm
Structure Panel: Lead	4100	8.02	0.00476
Structure Panel :Trail	1520	4.35	0.00138
Structure Panel: North	1320	2.50	0.00142
Structure Panel: South	1350	2.72	0.00146
Structure Panel: Space	1310	3.17	0.00146
Structure Panel: Earth	526	1.28	0.000557
Thrusters	746	1.65	0.000809
Antennas	5020	9.85	0.00544
Solar Array Cells	20900	50.8	0.0234
SAP Arms	376	0.809	0.000408

than 300 times higher for each component. Conversely, the impact frequency of particles larger than 1 mm was only 0.2% even on the solar array cells having the largest applicable to all exposed areas. This has only little effect on the functioning of the solar arrays, which proved to be robust against localized solar cell damage, but more vulnerable to penetration damages on the power harness on panel rear side [5]. The antennas also have higher impact risk given their relatively larger exposed areas. As a conclusion, it seems that an all-electric satellite should be designed with safety against particle impacts smaller than 1 mm.

#### 4 RISK ASSESSMENT BY PIRAT

The risk assessment described in Chapter 3 cannot consider the shielding effects by other components located around a focused component. Actually, some parts are located behind the structure panels, SAPs, and other components. The results shown in Tab. 2 may overestimate impact risks. Moreover, components installed inside the main structure are also subject to damage caused by the impacts of particles perforating the structure panel. The risks of damage to internal components cannot be estimated by the method used in Chapter 3. To assess impact risk, including shielding and perforating effects, this study used an impact risk assessment tool named Particle Impact Risk and vulnerability Analysis Tool (PIRAT) [6]. PIRAT can calculate the distribution of particle impact frequencies for a three-dimensional satellite model based on a debris environment model. A user can also analyze the impact risks of each component by applying ballistic limit equations. If a particle is judged to perforate a component, the effects of the perforating particle are also calculated for other components behind it. Impact risks of the internal structure can also be investigated. PIRAT version 2.2.1 was used for analysis in this study. Tab. 3 lists the material of each component.

##### 4.1 Risk Assessment Results

Figs. 4 and 5 show an example of the analysis results. The distribution of impact fluxes is indicated with colors on a

Table 3. Assumed Material of Each Component

Component	Material	Thickness
Structure Panel	MLI (0.2 kg/m <sup>2</sup> ) + CFRP Double Wall	CFRP Wall: 0.5 mm Stand-off: 20 mm
Antenna	CFRP Box	0.5 mm
SAP	CFRP Box	0.5 mm
SAP Arm	Aluminum Box	2.0 mm
Thruster	Titanium Cylinder	1.0 mm
Tank	Titanium Vessel	1.2 mm
Payload Box	Aluminum Box	1.0 mm

three-dimensional model. In both figures, the color contour ranges show different values. +X, +Y, and +Z show the leading, north, and zenith directions, respectively. In Fig. 4, the shielding effect by the antenna is observed on the structure panel. Impact fluxes on the thrusters installed on trailing side are smaller than those on the leading side thrusters. Fig. 5 shows the impact fluxes on internal components. Focusing on the boxes simulating payloads, their meshes located behind the antennas have low impact frequencies. Leading surfaces of the boxes indicate different flux values based on spacing distance from the leading structure panel. Greater spacing provides an expanding distribution area of fragments produced by a particle impacting the structure panel. Therefore, the number of impacts by fragments per unit area decreases with greater spacing. Analysis results by PIRAT express this effect. The payload attach fitting has a relatively high impact probability as its large parts are exposed in space. This satellite model has two plates near the structure panel facing the earth. These plates have been mounted where pipes and harnesses for the thrusters are set. The impact probability for these plates is also higher given their exposure to space.

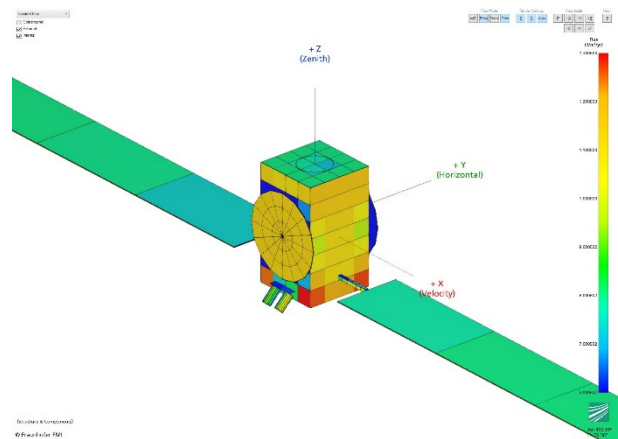


Figure 4. Flux Distribution on Outer Components

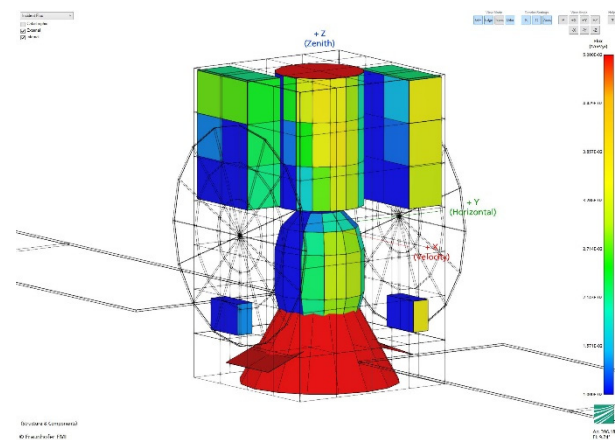


Figure 5. Flux Distribution on Internal Components

Fig. 6 shows the impact and perforation frequencies of each component during orbital transfer. The solar array cells and the antennas have perforation frequencies exceeding 1. As shown in Tab. 3, the SAPs and antennas were made of two CFRP plates to simulate a honeycomb sandwich panel. As the protection effect by a honeycomb core is not taken into consideration, the calculated perforation frequency are higher than actual. For the antennas, moreover, PIRAT recognizes a “perforation” when a particle has perforated through a front CFRP plate. The perforation of only a front CFRP plate does not mean the perforation of a sandwich panel. Thanks to their materials, the thrusters and SAP arms have lower perforation frequencies compared with their impact frequencies. As shown in Tab. 3, these components consist of metal plates. If the thicknesses are reduced or the material is changed to FRP, the change will be reflected in the sensitivity to perforation risk. The perforation frequency of internal components (boxes and tank) are quite low as the impact frequencies are also small. For internal components, the risk of failure caused by small debris impacts is considered low during orbit transfer.

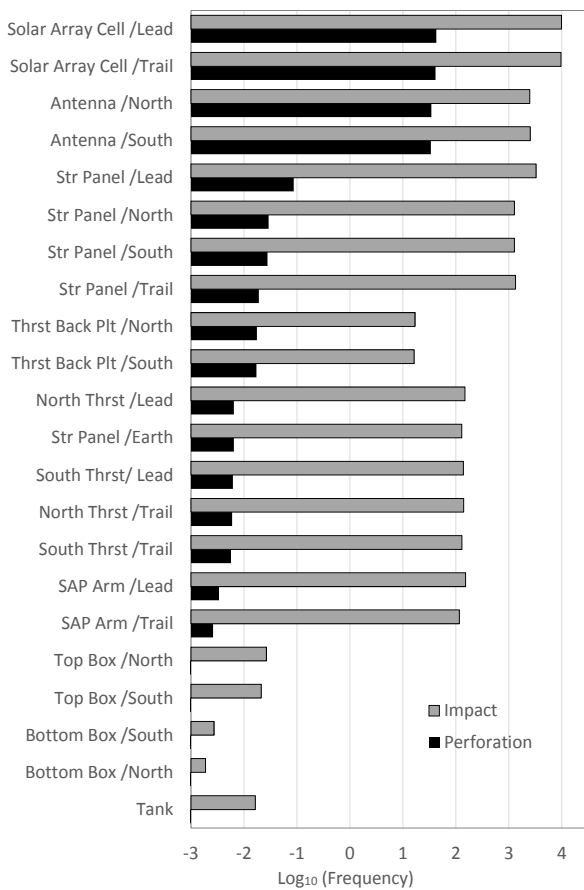


Figure 6. Impact and Perforation Frequencies of components of an electric propulsion satellite during orbit transfer

Next, the impact risk has been also analyzed for an orbit transfer with chemical propulsion by using the same orbit described in Chapter 3. Fig. 7 shows the particle impact frequencies and perforation risks of each component. No components of the chemical propulsion satellite have perforation probabilities exceeding 1. Except for the solar array cells and antennas, the perforation probability of each component is less than 0.2%. Impact risk assessment during orbit transfer is apparently unnecessary for a chemical propulsion satellite. In comparing Figs. 6 and 7, the average impact frequency of an electric propulsion satellite is about 55 times higher than that of a chemical propulsion satellite, and the average perforation risk of an electric propulsion satellite is about 54 times higher than that of a chemical propulsion satellite. These values are close to the ratio of increase in their orbit transfer durations. However, the perforation frequency of the tank has a relatively small increase ratio. Its perforation frequency of an electric propulsion satellite is about 42 times higher than that of a chemical propulsion satellite. The number of particles having high energy that can perforate the tank wall is considered lower when a satellite leaves low earth orbit.

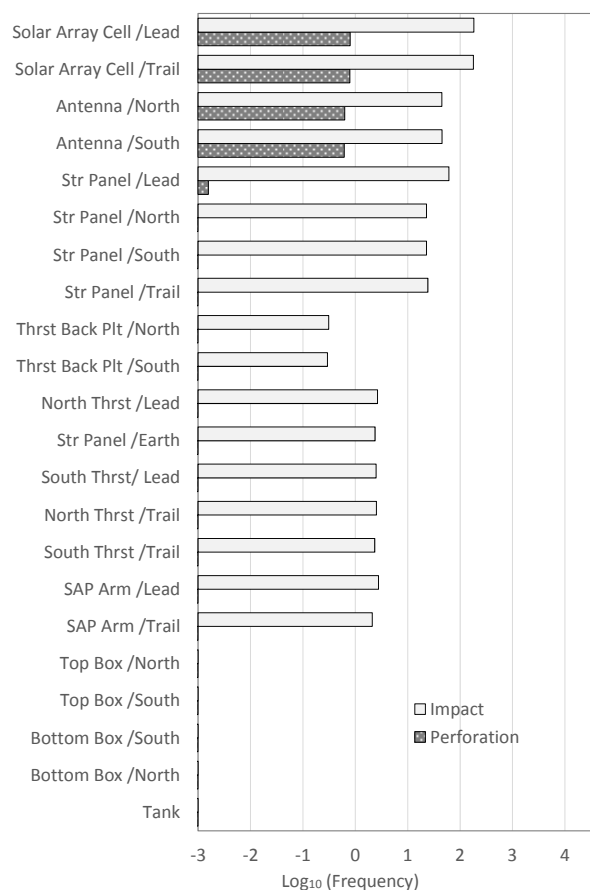


Figure 7. Impact and Perforation Frequencies of components of a chemical propulsion satellite during orbit transfer

## 4.2 Comparison with Risk Estimated from Single Surface Fluxes

To compare the impact risk analyzed by PIRAT as shown in Fig. 6 and estimated using single surface fluxes calculated by MASTER-2009 as shown in Tab. 2, the analysis results by PIRAT have been summarized for each component as shown in Tab. 4. For each component, the impact frequencies calculated by PIRAT are smaller than the estimation results obtained by using six single surfaces fluxes for particles greater than 1  $\mu\text{m}$  in diameter. In particular, the solar array cells and the leading structure panel show large differences between the estimation results obtained by using six single surfaces fluxes and PIRAT, which suggests that flux is shadowing the structure panel and the SAPs. The analysis of impact frequency by PIRAT can include the shielding effects by other components. Impact frequency estimations based only on MASTER-2009 flux data show safety side results; however, an overestimation could result.

Next, the risks of perforation are compared. For the structure panels, the impact frequencies estimated from six single surfaces fluxes for particles larger than 1 mm are closest to the risk calculated by PIRAT. Perforations by particles 0.1 to 1 mm in size are implied, and are in good agreement with past impact experiment results for CFRP honeycomb sandwich panels [7,8]. For the thrusters as well, the impact frequencies of particles larger than 1 mm show the closest value to the calculated perforation risk. In contrast, for the antennas and the solar array cells, the impact frequencies of particles larger than 0.1 mm show the closest value to the calculated perforation risk. As previously described, the impact frequencies estimated from single surface fluxes are overestimated as shadowing effects are not included. Therefore, the results shown in Tab. 4 suggest that particles larger than 0.1 mm cause perforation of the solar array cells, even though it may not be true.

Table 4. Impact and Perforation Frequencies of Each Component Calculated by PIRAT

Component	Impact Frequency	Perforation Frequency
Structure Panel: Lead	3270	0.0869
Structure Panel :Trail	1340	0.0191
Structure Panel: North	1280	0.029
Structure Panel: South	1270	0.0277
Structure Panel: Space	1220	0.0266
Structure Panel: Earth	162	0.00645
Thrusters	559	0.0243
Antennas	5020	68.4
Solar Array Cells	19500	84.1
SAP Arms	269	0.00601

## 5 SUMMARY

To assess the non-catastrophic collision risk for an all-electric satellite, this study investigated the small debris impact risk of a satellite during orbit transfer from GTO to GEO.

Impact flux was calculated by MASTER-2009. The frequency of particle impacts on a satellite during orbit transfer was found to depend on the duration of transfer. Compression of the duration reduces risk of impact damage. Particles smaller than 1 mm were found to have collision possibility on components an all-electric satellite during orbit transfer.

By using a 3-dimensional satellite model bus, risk analysis for each component was conducted by PIRAT. The perforation frequencies of solar array cells and antennas exceeded 1 for the model used in this study. Thrusters had low perforation frequency, but were found to vary sensitively by the material applied, given their relatively high impact frequency. Since the failure risks of internal components were low, impact risk of sub-millimeter objects on the outer components is supposed to be taken into consideration for designing an all-electric satellite. Risk analysis for a satellite with conventional chemical propulsion was also conducted. As a result, risk assessment was deemed unnecessary for chemical propulsion transfer.

Component risks calculated by PIRAT were compared with risks estimated from single surface fluxes calculated by MASTER-2009. The estimation of risk showed a safety side, but was overestimated as the shadowing effects of other components had not been taken into consideration.

In conclusion, risk of non-catastrophic failure caused by small debris impacts is considered low during orbit transfer, even if a satellite spends 6 months transferring.

## REFERENCES

1. Polk, M., Woods, D., Roebuck, B., Opiela, J., Sheaffer, P. & Liou, J.-C. (2005). Orbital Debris Assessment Testing in the AEDC Range G. *Procedia Eng.* **103**, 490-498.
2. Hanada, T. & Liou, J.-C. (2008). Comparison of Fragments Created by Low- and Hyper-Velocity Impacts. *Adv. Space Res.* **41**(7), 1132-1137.
3. Putzar, R., Schäfer, F., Stokes, H., Chant, R. & Lambert, M. (2005). Vulnerability of Spacecraft Electronics Boxes to Hypervelocity Impacts. In *Proc. 56th IAC*.
4. Kawakita, S., Segami, G., Nitta, K., Kusawake, H., Takahashi, M., Matsumoto, H. & Hasegawa, S. (2009). Discharge of Spacecraft Solar Panels by Hypervelocity Impact. *Trans. JSASS Space Tech. Japan.* **7**(ists26), Tr\_2\_53-Tr\_2\_56.

5. Schimmerohn, M., Rott, M., Gerhard, A., Schäfer, F. & D'Accolti, G. (2014). Susceptibility of Solar Arrays to Micrometeoroid and Space Debris Impact. In *Proc. 10th Europ. Space Power Conf*, ESA SP-719.
6. Kempf, S., Schäfer, F., Cardone, T., Ferreira, I., Gerené, S., Destefanis, R. & Grassi, L. (2016). Simplified Spacecraft Vulnerability Assessments at Component Level in Early Design Phase at the European Space Agency's Concurrent Design Facility. *Acta Astronautica*. **129**, 291–298.
7. Higashide, M., Nagao, Y., Kibe, S., Francesconi, A. & Paverin, D. (2010) Debris Impact on CFRP-AL Honeycomb Sandwich Structure. *Trans. JSASS Space Tech. Japan*. **8**(ists27), Pr\_2\_1-Pr\_2\_5.
8. Ryan, S., Schäfer, F., Destefanis, R. & Lambert, M. (2008). A Ballistic Limit Equation for Hypervelocity Impacts on Composite Honeycomb Sandwich Panel Satellite Structures. *Adv. Space Res.* **41**(7), 1152-1166.